

Histone H4K20 Trimethylation Is Decreased in Murine Models of Heart Disease

Samuel M. Hickenlooper,^{*,#} Kathryn Davis,[#] Marta W. Szulik, Hanin Sheikh, Mickey Miller, Steven Valdez, Ryan Bia, and Sarah Franklin^{*}



Cite This: *ACS Omega* 2022, 7, 30710–30719

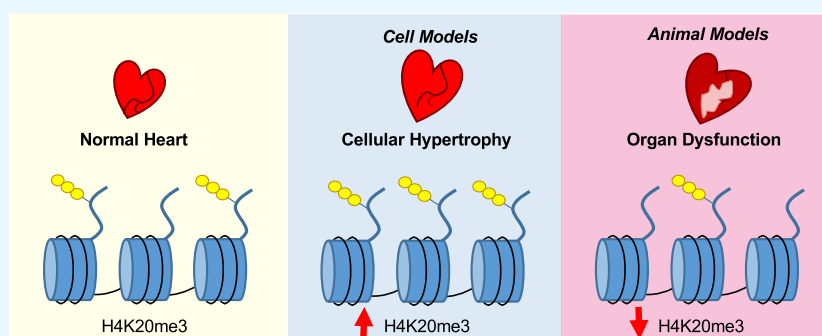


Read Online

ACCESS |

Metrics & More

Article Recommendations



ABSTRACT: Heart disease is the leading cause of death in the developed world, and its comorbidities such as hypertension, diabetes, and heart failure are accompanied by major transcriptomic changes in the heart. During cardiac dysfunction, which leads to heart failure, there are global epigenetic alterations to chromatin that occur concomitantly with morphological changes in the heart in response to acute and chronic stress. These epigenetic alterations include the reversible methylation of lysine residues on histone proteins. Lysine methylations on histones H3K4 and H3K9 were among the first methylated lysine residues identified and have been linked to gene activation and silencing, respectively. However, much less is known regarding other methylated histone residues, including histone H4K20. Trimethylation of histone H4K20 has been shown to repress gene expression; however, this modification has never been examined in the heart. Here, we utilized immunoblotting and mass spectrometry to quantify histone H4K20 trimethylation in three models of cardiac dysfunction. Our results show that lysine methylation at this site is differentially regulated in the cardiomyocyte, leading to increased H4K20 trimethylation during acute hypertrophic stress in cell models and decreased H4K20 trimethylation during sustained ischemic injury and cardiac dysfunction in animal models. In addition, we examined publicly available data sets to analyze enzymes that regulate H4K20 methylation and identified two demethylases (KDM7B and KDM7C) and two methyltransferases (KMT5A and SMYD5) that were all differentially expressed in heart failure patients. This is the first study to examine histone H4K20 trimethylation in the heart and to determine how this post-translational modification is differentially regulated in multiple models of cardiac disease.

INTRODUCTION

Heart disease is the leading cause of death throughout the world.¹ Precursors to heart disease include common conditions such as diabetes and hypertension. These persistent stressors can lead to large changes in the cardiac morphology and often cause many types of cardiac dysfunction including heart failure. It has also been shown that many cardiac pathologies result from dynamic changes in gene expression and conversely that modulating epigenetic factors in murine models can prevent or abrogate ischemic injury and pathological remodeling.² For example, during cardiac hypertrophy and failure, there is a global upregulation of genes more commonly involved in heart development.³ These largescale transcriptome changes are preceded by epigenetic alterations to chromatin.

Chromatin contains DNA wrapped around an octamer of histone proteins (two copies each of H2A, H2B, H3, and H4), which have N-terminal tails that extend beyond the core protein structure and interact with a large number of regulatory proteins.⁴ Transcription can be activated or silenced depending on the chromatin environment: for example, more accessible euchromatin allows transcription factors and other transcrip-

Received: February 18, 2022

Accepted: July 6, 2022

Published: August 23, 2022



Table 1. Enzymes That Regulate H4K20 Methylation^a

gene ID	synonyms	enzymatic activity	histone target
KMT5A	SET8 ^{H,M} and PR-SET7 ^D	methyltransferase	H4K20me1
MMSET	NSD2 ^{H,M}	methyltransferase	H4K20me2
KMT5B	SUV4-20H1 ^{H,M}	methyltransferase	H4K20me2/me3
KMT5C	SUV4-20H2 ^{H,M}	methyltransferase	H4K20me2/me3
SMYD3	ZMYND1 ^Z and ZNFN3A1 ^Z	methyltransferase	H4K20me3
SMYD5	RAI15 ^H	methyltransferase	H4K20me3
KDM7B	JHDM1F ^{H,M} /PHF8 ^{H,M} /KIAA1111 ^{H,M} /ZNF422 ^H	demethylase	H4K20me1
LSD1n	KDM1An ^H	demethylase	H4K20me2
KDM9	RSBN1 ^{H,M} /KIAA3002 ^M /DPY-1 ^Y	demethylase	H4K20me2
RAD23A	hHR23A ^H	demethylase	H4K20me2/me3
RAD23B	hHR23B ^H	demethylase	H4K20me2/me3
KDM7C	JHDM1E ^{H,M} /PHF2 ^{H,M} /KIAA0662 ^{H,M} /CENP-35 ^H /GRCS ^{H,M} (protein)	demethylase	H4K20me3

^aH = human, M = mouse, D = drosophila, Y = yeast, and Z = zebrafish.

tional machinery to bind chromatin, while less accessible heterochromatin prevents this binding and silences gene expression.⁵ One epigenetic mechanism that contributes to the chromatin landscape and gene expression is the post-translational modification (PTM) of histone proteins.^{6,7} Histones are subject to a wide number of PTMs including the methylation of arginine (R) and lysine (K) residues. Regarding lysine methylation, this amino acid can be reversibly methylated and can accept up to three methyl groups (mono-, di-, or tri-methylation, respectively, abbreviated as me1, me2, and me3).^{6,8} Sites of lysine methylation, including K4 and K9 on histone H3, were among the first methylated lysine residues to be identified⁹ and have been linked to gene activation and silencing, respectively. While these two residues have been a main focus of research regarding lysine methylation and its role in transcriptional regulation, much less is known regarding other methylated lysine residues. Among the less studied modifications is histone H4K20 methylation.

The methylation of histone H4K20 was first discovered by DeLange et al., who examined residues of histone tails in calf and pea extracts; however, the exact function of this histone modification, also known as a histone mark or a methyl mark, was not known at the time.¹⁰ Three decades later, the first reports were published that linked specific methyltransferases responsible for methylation of histone H4 at lysine K20 together with functional studies that revealed the effects of histone H4K20 methylation on the chromatin status and transcriptional regulation of genes.¹¹ In general, methylation of H4K20 has been implicated in gene silencing, heterochromatin formation, mitosis, and genomic stability.^{12,13} More specifically, mono- and di-methylation of H4K20 are marks found on active genes implicated in cell cycle regulation and DNA repair,¹⁴ while trimethylation is most often associated with heterochromatin formation and gene repression.¹² Most commonly, H4K20me3 is located at gene promoters and functions to repress transcription alongside specific chromatin readers. Each of these methylation states are carried out by separate enzymes called lysine methyltransferases, and these methyl marks are selectively removed by lysine demethylases (Table 1).¹⁵ Notably, there are only seven enzymes (of a total of 12 that modify histone H4K20 methylation) that catalyze or remove H4K20 trimethylation that have been identified to date (visualized in Figure 1) compared to 16 total enzymes that regulate H3K4 trimethylation.¹⁶ This suggests that there may be other enzymes that regulate H4K20 trimethylation that have not been identified to date. While we are beginning to

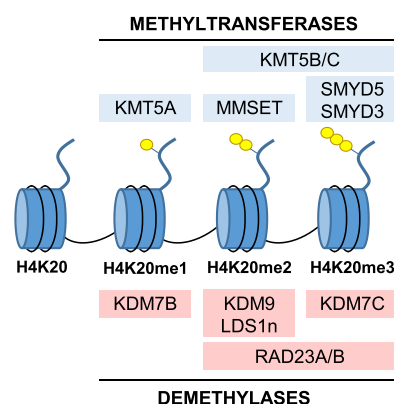


Figure 1. Enzymes that regulate H4K20 methylation. There are relatively few enzymes known to regulate H4K20 methylation. Blue boxes indicate methyltransferases that catalyze each methylation state. Red boxes indicate demethylases that remove specific methyl marks from H4K20 in the sequential order (yellow circles depict H4K20 methylation).

understand the complexity of these methylation marks and the diverse processes they regulate, much less is known regarding their role in specific cell types and pathologies. Along these lines, the methylation of histone H4K20 has never been examined in the heart or cardiomyocytes.

Analysis of global changes in histone PTMs (vs methylation on specific genes) can provide insights into how the transcriptome changes in response to stress or disease. Presently, there have only been three studies that have examined the total abundance of histone methylation in the context of heart disease. These studies examined histone H3K4me3,^{17,18} H3K9me3,^{17,18} and H3K36me3¹⁹ in human heart failure patients and rodent models of heart failure and showed global increases in H3K4me3 abundance and decreases in H3K9me3 in the cardiac tissue.^{17,18} In addition, studies in both rats and humans used CHIP-Seq-based profiling to show that the genomic regions containing each of these three specific histone modifications change substantially in failing hearts compared to that in healthy donor controls, indicating a significant shift in which genes are being actively transcribed.^{17,19} These results suggest that the modulation of histone methylation is important in the development and progression of heart disease. However, studies regarding other sites of methylation on histones, including H4K20me3, have not been examined in the healthy or diseased heart.

In this study, we utilized both cell and animal models of cardiac dysfunction to examine histone H4K20 trimethylation abundance during disease. We focused on H4K20 trimethylation, a known repressive histone mark, rather than the other methylation states of H4K20 due to our interest in transcriptional regulation of genes in cardiomyocytes. Cardiomyocytes are terminally differentiated and thus exit the cell cycle, which is generally regulated by mono- and dimethylation of H4K20; therefore, we did not examine these histone marks. Our results show that H4K20 trimethylation is increased in isolated cardiomyocytes during acute hypertrophic stress but is decreased in the heart after long-term exposure to isoproterenol (ISO) or ischemic injury in mice. In addition, we profiled public databases of methyltransferases and demethylases, which regulate histone H4K20 methylation, to determine which of these enzymes are differentially expressed in human heart failure patients. Specifically, we identified two demethylases (KDM7B and KDM7C) and two methyltransferases (KMT5A and SMYD5) that were differentially expressed in heart failure patients. Of these four enzymes, only SMYD5 and KDM7C are known to regulate trimethylation of H4K20, suggesting that these enzymes may be responsible for the methylation changes observed at this site in the heart. This is the first study to examine histone H4K20 trimethylation in the heart and to determine how this PTM is differentially regulated in multiple models of cardiac disease.

METHODS

Mouse Models of Cardiac Stress. All protocols involving animals conform to the NIH Guide for the Care and Use of Laboratory Animals and were approved by the Institutional Animal Care and Use Committee of the University of Utah. All efforts were made to minimize pain and distress during procedures and isolation of the heart by anesthesia. In this study, we used both male and female FVB mice.

ISO Treatment of Mice. FVB mice between the age of 8–12 weeks were treated with ISO (15 mg/kg/d) via subcutaneous implantation of osmotic mini-pumps (Alzet 2004) for 6 weeks, as previously described.^{20,21} Briefly, pumps were prepared before implantation by filling the reservoir with sterile ISO solution (saline was used as a control). Mice were anesthetized, and the subcutaneous tissue on the back was spread apart by inserting a hemostat to create enough room for the pump. The filled pump was inserted and kept clear of vital organs and the incision. The incision was closed using a sterile suture. Mice were monitored weekly by echocardiography (ECHO) to assess cardiac function (as detailed below). Cardiac tissue was harvested after 6 weeks, weighed, and used for downstream analyses.

Ischemic Injury via Left Anterior Descending Coronary Artery Ligation. The left anterior descending coronary artery (LAD) was ligated in FVB mice as reported previously with minor modifications.²² Briefly, mice were put under mechanical ventilation with anesthesia, and the chest was opened through a left thoracotomy. A suture was placed around the LAD coronary artery, as it emerges from under the left atrium, to permanently occlude the LAD. The sham control group underwent the same surgical procedure without ligation of the LAD. Mice were monitored weekly by ECHO to assess cardiac function (as detailed below). Mice were sacrificed 48 h and 3 weeks after LAD ligation, and cardiac tissue was excised, weighed, and used for downstream analyses.

Echocardiography. ECHO was used to monitor the physiological and functional parameters of the heart using a Vevo 770 high-resolution ECHO system coupled to a 35 MHz transducer. Mice were sedated with 1% isoflurane, and ECHO was performed weekly on all experimental animals, pre- and post-surgery, for evaluation of cardiac function, including the ejection fraction (EF), using the short- and long-axis views.

Histology. Hearts were excised and fixed in 4% paraformaldehyde and then embedded in paraffin. Hearts were then sectioned into five slices from the apex to the base and placed on slides. Hematoxylin and eosin staining (H/E) and Masson's trichrome (Sigma) staining were performed by the Huntsman Cancer Institute Biorepository and Molecular Pathology Research Histology Core. Tissue sections were visualized and imaged on an Olympus BX51WI microscope using cellSens Standard software (Olympus).

Cultured H9c2 Cells (Rat Cardiomyoblasts). H9c2 cells were cultured in Dulbecco's modified Eagle medium (DMEM) supplemented with 10% fetal bovine serum (FBS) and 1% penicillin–streptomycin (P/S) until 80% confluent. Cells were then differentiated in DMEM supplemented with 1% FBS and 1% P/S for 48 h. To induce hypertrophic growth, cells were treated with 100 μ M phenylephrine (PE) for 48 h and then harvested for experiments.

Cultured 3T3 Mouse Fibroblasts. 3T3 fibroblasts were cultured in DMEM supplemented with 10% FBS and 1% P/S until 80% confluent. To compare histone methylation in these cells to that in cardiomyocyte cells in hypertrophic stress, they were similarly treated with 100 μ M PE, 100 μ M ISO, or 100 nM endothelin-I (ET-1) for 48 h and then harvested for experiments.

Western Blotting. Protein samples were diluted in Laemmli buffer, resolved on 12% SDS-PAGE gels, and then transferred to nitrocellulose membranes using the semi-dry transfer method (Bio-Rad), as we have previously published.^{23,24} The success of protein transfer to the membrane was confirmed using Ponceau S (0.1% w/v in 5% acetic acid). These membranes were blocked with either 5% powdered bovine milk reconstituted in TBS-T (1X Tris-buffered saline, 0.1% Tween-20) or 5% BSA (bovine serum albumin) in TBS-T, depending on the suggestions from the manufacturer (Abcam). Antibodies used in this study are as follows: histone H4K20me3 (Abcam, ab9053), histone H4 (Abcam, ab10158), β -tubulin loading control (Abcam, ab6046), and goat anti-rabbit (Abcam, ab97051). Statistical significance was determined by Student's two sample *t*-test (*p*-value < 0.05).

Quantitative Real-Time PCR Analysis. Total RNA was isolated with Trizol according to the manufacturer's instructions, as we have previously published.²⁵ cDNA was synthesized using the Superscript III First Strand Synthesis System (Life Technologies), and PCR was performed using a Bio-Rad CFX Connect RT-PCR detection system. The primers used were for *Nppa*, Natriuretic Peptide A, (FWD: CTGATGGATTTCAAGAACCCTGCT and REV: CTCTGGGCTCCAATCCTGTC) as a marker of cardiac stress and myocyte hypertrophy and *β -Actin* (FWD: GGGGTGTTGAAGGTCTCA and REV: TGTTACCAACTGGGACGA) as a housekeeping gene. Statistical significance was determined by Student's two sample *t*-test (*p*-value < 0.05).

Liquid Chromatography Tandem Mass Spectrometry. Sample preparation for mass spectrometry was performed using a standard FASP protocol that we have previously

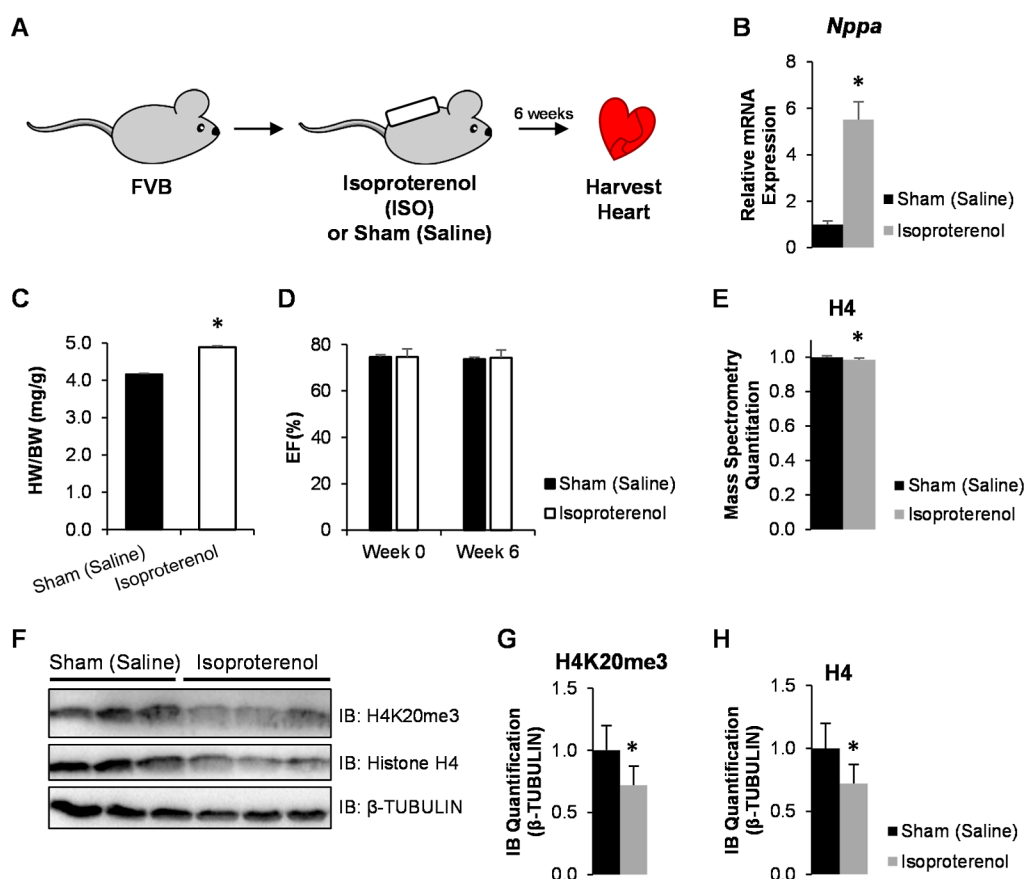


Figure 2. Decreased H4K20 trimethylation and histone H4 in the mouse heart after ISO-induced cardiomyopathy. (A) Mice were treated with ISO via mini-osmotic pump implantation or saline (control) for 6 weeks. ($n = 3$) (B) Cardiac stress was confirmed by quantifying *Nppa* via RT-qPCR, (C) heart weight to body weight ratios (HW/BW) in milligrams per gram of sham- and ISO-treated mice, and (D) EF (EF %) measured pre-pump implantation and measured 6 weeks after treatment. (E) Mass spectrometry quantitation of histone H4 in both groups. (F) Immunoblot analysis of cardiac tissue from these animals showed a decrease in (G) histone H4K20 trimethylation and (H) histone H4 (both normalized to β -Tubulin). Asterisk indicates a p -value of <0.05 .

published.¹⁸ Samples were diluted with urea buffer, reduced, and alkylated, and then, proteins were digested with trypsin overnight at 37 °C and acidified using 1% formic acid.

Peptides were analyzed using an Orbitrap Velos Pro mass spectrometer (Thermo Scientific) interfaced with an Easy nLC-1000 ultrahigh-performance liquid chromatograph and outfitted with an ESI Source Solutions pulled tip column type 2 (15 cm \times 75 μ m inner diameter, 3 μ m particle size, and 120 Å pore diameter, ESI Source Solutions). Spectra were acquired in the data-dependent mode with dynamic exclusion enabled, and peptides were fragmented using CID fragmentation. The top 20 MS1 peaks were analyzed at a resolution of 30,000. Samples were run in duplicate to generate technical replicates.

The resulting spectra were analyzed using MaxQuant 1.6.7.0 against the UniprotKB mouse protein database. Search engine parameters for MaxQuant were as follows: trypsin digestion, two missed cleavages, a precursor mass tolerance of 20 ppm, and a fragment mass tolerance of 0.5 Da. Match between runs was enabled with a match time window of 0.3 min, a match ion mobility window of 0.05, and an alignment time window of 20 min. The false discovery rate (FDR) was 1%. Quantification of histone H4 by mass spectrometry was performed using MaxQuant label free quantitation (as has been previously published).²⁶ Statistical significance was determined by Student's two sample t -test (p -value < 0.01), and statistical analyses were performed in Perseus 1.6.5.0. The mass

spectrometry proteomics data have been deposited to the PRIDE Archive (<http://www.ebi.ac.uk/pride/archive/>) via the PRIDE partner repository with the data set identifier PXD031617.

RESULTS

ISO Treatment in Mouse Hearts Leads to Decreases in H4K20 Trimethylation. Cardiac dysfunction is preceded by large transcriptomic changes within the heart, which presumably involves changes in histone PTMs. To examine whether H4K20 trimethylation levels change in the diseased heart, we first examined the cardiac tissue from mice after ISO treatment, which is a β -adrenergic receptor agonist that induces cardiac hypertrophy and failure.²⁷ This model mimics nonischemic cardiomyopathy (NICM), as seen by chronic adrenergic stimulation due to elevated catecholamine levels, in heart failure patients.^{21,28} We implanted mice with ISO-filled osmotic mini-pumps that allows continuous diffusion of ISO, or saline as a control, over the course of 6 weeks (Figure 2A). At this time point, ISO-treated mice were experiencing cardiac hypertrophy, confirmed by the increased expression of *Nppa*, an established marker of cardiac hypertrophy, in the heart via qPCR (Figure 2B), and increased heart weight to body weight ratios (Figure 2C). EF analysis showed no change in the overall heart function (Figure 2D).²⁹ We also quantified changes in histone H4K20 trimethylation in the cardiac tissue

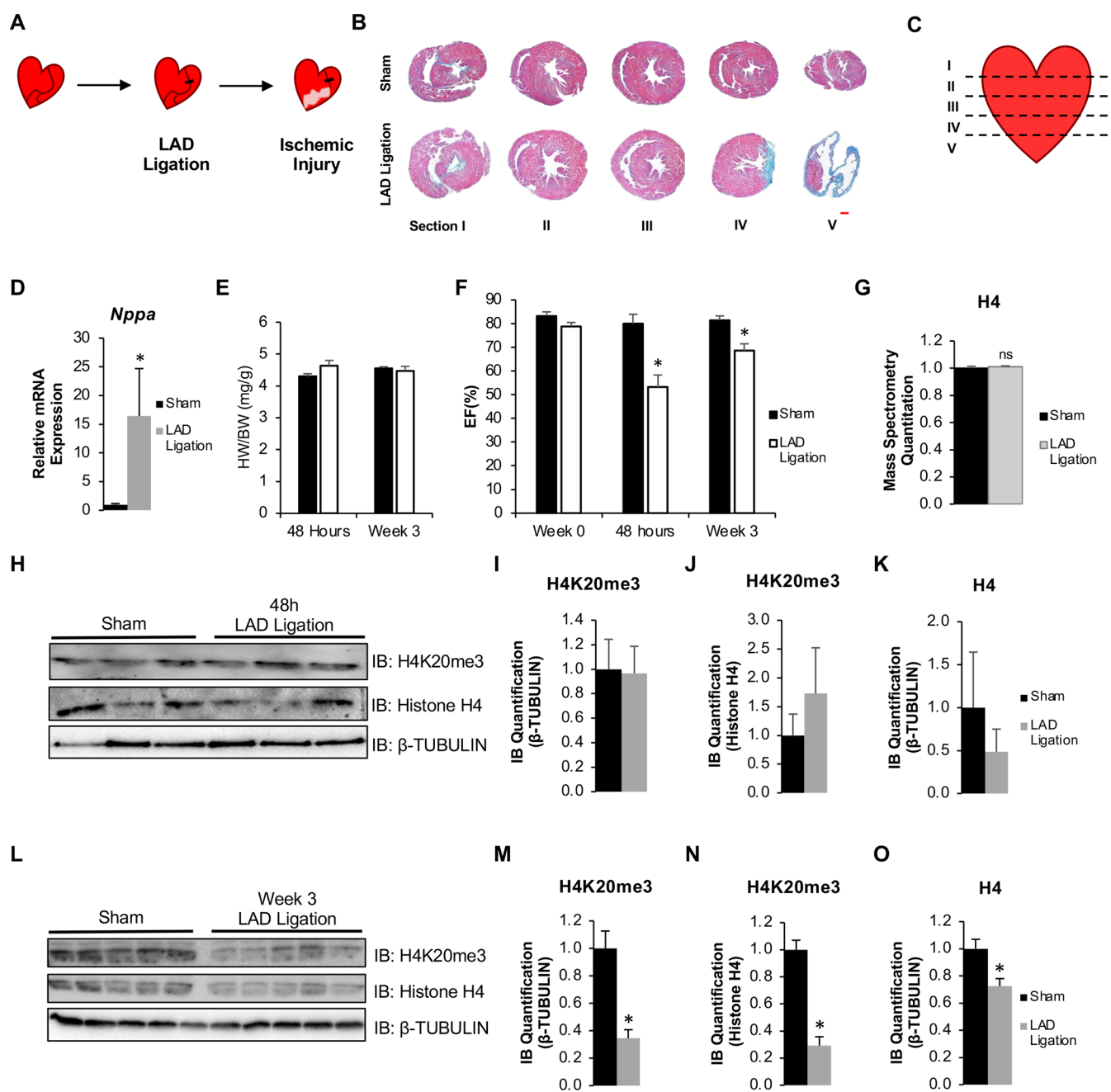


Figure 3. Decreased H4K20 trimethylation in the mouse heart after ischemic injury. (A) Mice were subjected to ischemic injury by ligating the LAD coronary artery. Sham surgery was used as a control where no ligation was performed. ($n = 5$) (B) Representative histological analysis of sections I through IV collected from LAD samples. Scale bar in red, 200 pm. (C) Representation cartoon of the sectioned heart to show that section III is collected for western blot analysis. (D) Cardiac tissue was excised and *Nppa* was quantified via RT-qPCR to confirm cardiac dysfunction. (E) Heart weight to body weight (HW/BW) ratios from sham and experimental groups in milligrams per gram. (F) EF (EF %) from sham and experimental groups pre-ligation and either 48 h post ligation or 3 weeks post-ligation. (G) Global abundance of histone H4 calculated by mass spectrometry. (H) Immunoblotting of cardiac tissue 48 h post-ligation shows no significant changes in H4K20 trimethylation when normalized to (I) β -Tubulin or (J) histone H4 abundance. (K) Immunoblotting of histone H4 normalized to β -Tubulin shows no change. (L) Immunoblotting of cardiac tissue 3 weeks post-ligation showed a decrease in H4K20 trimethylation when normalized to (M) β -Tubulin or (N) histone H4 abundance. Global abundance of histone H4 was decreased in cardiac tissue when examined by (O) immunoblotting. Asterisk indicates a p -value of <0.05 . (ns = not significant).

and observed a $\sim 30\%$ decrease in abundance in the ISO-treated group (Figure 2F,G). Because of two key reasons, we decided to quantify histone H4 abundance using an additional technique (via mass spectrometry): (1) PTMs have been reported to affect the efficiency of antibody binding in an antibody-based assay³⁰ and (2) previous reports have

suggested that global histone H4 levels are regulated at both the transcriptional and post-transcriptional levels to keep them uniquely stable and tightly controlled.³¹ Thus, we quantified global histone H4 abundance via mass spectrometry (Figure 2E) and western blotting (Figure 2H) and found significant

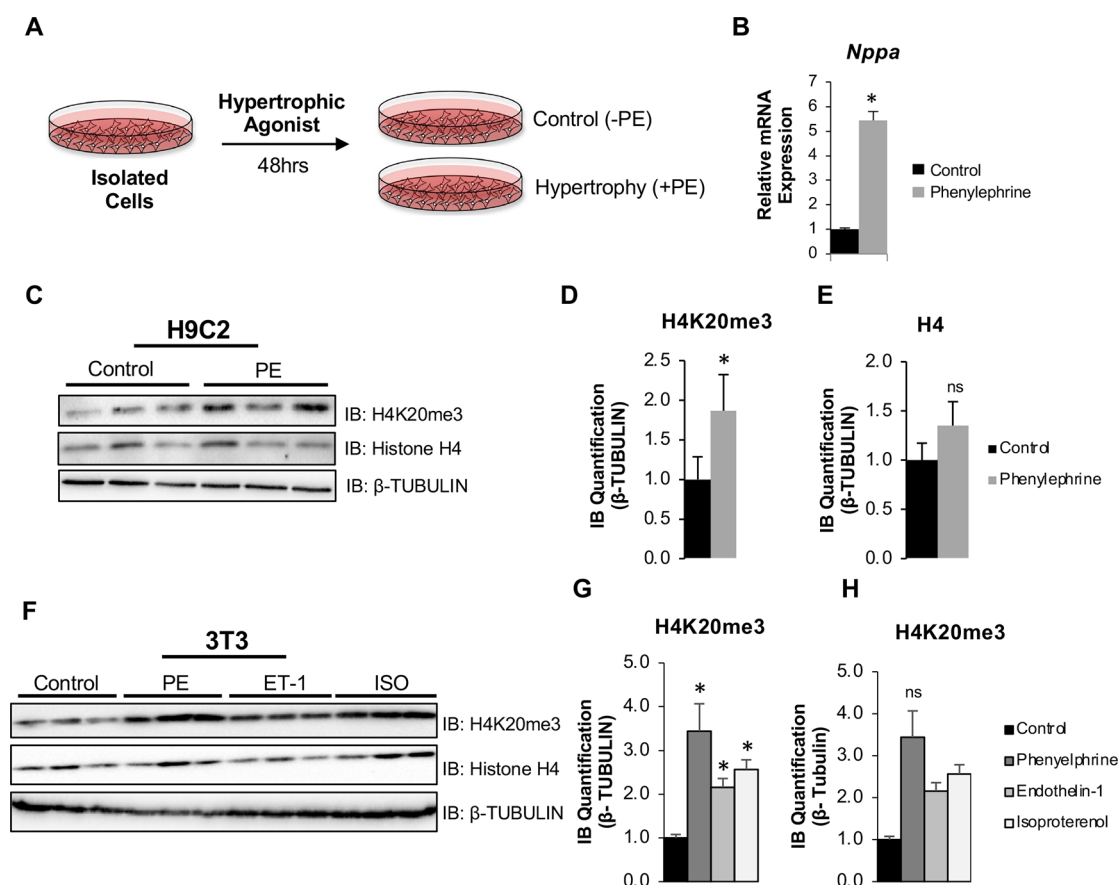


Figure 4. Acute hypertrophy in isolated cells increases H4K20me3 abundance. (A) Cultured cardiomyocytes (H9c2 cells) and 3T3 fibroblasts were treated with PE or other hypertrophic agents for 48 h. ($n = 3$ per condition) (B) Relative expression of *Nppa* in H9c2 cells via RT-qPCR confirmed hypertrophic treatment. (C) Immunoblotting of H9c2 cell lysates showed an increase in (D) histone H4K20 trimethylation with no change in (E) total histone H4 abundance (both normalized to β -tubulin). (F) Immunoblotting of 3T3 cell lysates after 48 h treatment of PE, ET-1, and ISO showed an increase in (G) histone H4K20 trimethylation with no change in (H) total histone H4 abundance (both normalized to β -tubulin). Asterisk indicates a p value of <0.06 . (ns = not significant)

decreases in experimental animals compared to that in controls.

Ischemic Injury via LAD Ligation in Mice Results in Decreased H4K20 Trimethylation. To evaluate levels of histone H4K20me3 in a different mouse model, we performed permanent ligation of the LAD on mice, a surgery that mimics ischemic cardiomyopathy (ICM) via myocardial infarction,³² and followed them for either 48 h or 3 weeks post-ligation (Figure 3A). After the hearts were excised, they were divided into five separate sections (Figure 3B), from which section III was utilized for western blotting (Figure 3C). Evaluation of *Nppa*, a known marker of cardiac hypertrophy and failure, showed a 15-fold increase in experimental groups compared to sham controls (Figure 3D). We also measured heart weight to body weight ratios; however, as expected, we found no significant changes in any group due to hypertrophic compensation of the tissue near the base of the heart in response to necrosis at the apex (Figure 3E). To further confirm cardiac dysfunction, we evaluated cardiac function via ECHO and found decreased EF (EF %) in experimental animals after both 48 h and 3 weeks post-ligation (Figure 3F). Then, we examined the abundance of histone H4K20me3 and total histone H4 via western blotting, which had no significant changes at the 48 h time point (Figure 3H–K); however, decreased expressions by ~70% and 30% were observed at the 3 weeks post-ligation compared to sham controls, respectively

(Figure 3L–O). Quantification of histone H4 by mass spectrometry using MaxQuant label free quantitation (as has been previously published)²⁶ showed no significant change in abundance (Figure 3G).

PE-Induced Hypertrophy in Isolated Cardiomyocytes Increases H4K20 Trimethylation. To investigate whether histone H4K20 trimethylation changes in a cell model of hypertrophy, we cultured H9c2 cells (cardiomyoblasts), differentiated them in low-serum media to confer a more cardiomyocyte-like phenotype, and treated them with PE, an α -adrenergic receptor agonist (Figure 4A). After 48 h, we observed an increased expression of *Nppa* (~5-fold) in the treated cells (Figure 4B). Quantification of histone H4K20 trimethylation in these cells (Figure 4C–E) showed a 1.8-fold increase with no significant change in histone H4 abundance in treated cells. After examining isolated cardiomyocytes, we also wanted to examine the other major cell population present in the heart, specifically fibroblasts, to determine whether these non-cardiac cells had an impact on the overall H4K20 trimethylation abundance in the heart during hypertrophy. We treated fibroblasts with pharmacological agents to examine changes in H4K20 trimethylation after PE, ET-1, and ISO treatment. We chose multiple pro-hypertrophic agents to examine whether these different stressors elicited unique or consistent responses in fibroblasts. Our results show a significant increase in H4K20 trimethylation in all models

Table 2. H4K20 Methyltransferases and Demethylases Differentially Expressed in Human Cardiac Disease^a

gene ID	all known histone targets	ICM	NICM	DCM	HF	cardiac KO/KD phenotype
<i>KMT5A/SET8/PR-SET7</i>	H4K20me1	+1.2 ³⁵				unknown
<i>KDM7B/PHF8/JHDM1F</i>	H4K20me1				-1.536	mouse: inhibits cardiac hypertrophy upon pressure overload ³⁶
<i>KDM7C/PHF2/JHDM1E</i>	H3K9me1/me2, H4K20me3	+1.43 ³³		+2.2 ³⁵		unknown
<i>SMYD5</i>	H4K20me3		+1.2 ³⁴			zebrafish: normal cardiac development ³⁷

^aEnzymes that are differentially expressed in human cardiac disease. Values indicate the fold change for transcripts with a *p*-value < 0.05. A negative value corresponds to downregulated transcripts, and a positive value corresponds to upregulated transcripts. ICM, ischemic cardiomyopathy; NICM, nonischemic cardiomyopathy; DCM, dilated cardiomyopathy; and HF, heart failure of unknown cause.

with no significant change in histone H4 abundance (Figure 4F–H).

Enzymes That Regulate H4K20 Methylation Are Differentially Expressed in Human Heart Failure. The changes we observed in histone H4K20 methylation in the cardiac tissue must be accomplished by the enzymes that regulate these methyl marks, primarily lysine methyltransferases and demethylases. Therefore, we examined processed data from publicly available data sets from three separate studies that analyzed transcript expression in cardiac tissue from patients experiencing ICM, NICM, or dilated cardiomyopathy (DCM), Sweet et al.,³³ Yang et al.,³⁴ and Liu et al.³⁵ For each study, statistical significance was determined on an individual study basis using the filters published within the specific study. In the first study, Sweet et al. determined the statistical significance of RNA sequencing based on filters, which included differentially expressed genes (DEGs) defined as genes with a difference in reads per kilobase of the transcript, per million mapped reads (RPKM) between groups ≥ 5 , and a *p*-value adjusted for the Benjamini–Hochberg FDR ≤ 0.05 .³³ In the second study, Yang et al. used specific filters described in the study that determined statistical significance of microarray and RNA sequencing of heart samples via the paired sample Wilcoxon signed rank test, where a two-tailed *p*-value < 0.05 was considered statistically significant.³⁴ Finally, Liu et al. used their own unique filters for their RNA sequencing data obtained from human heart tissue, which utilized statistical significance as a fold change equal to or greater than 1.2 with a *p*-value less than 0.05.³⁵ In these studies, we found only three enzymes that regulate H4K20 methylation, and they were differentially expressed in at least one disease condition (Table 2). Specifically, one demethylase, *KDM7C*, was upregulated 1.43-fold in ICM and 2.2-fold in DCM, and two methyltransferases (*KMT5A* and *SMYD5*) were upregulated 1.2-fold in ICM and NICM, respectively. One additional study examined failing human hearts (type of cardiomyopathy unknown) explanted during transplantation (*n* = 4) and found that *KDM7B*, an H4K20me1-specific demethylase, was significantly downregulated via western blotting and qPCR compared to that in non-failing donor hearts.³⁶

We also examined publicly available data sets compiled for murine models of heart failure; however, these studies did not report significant changes in the expression of the H4K20-specific methyltransferases or demethylases in microarrays or RNA sequencing.³⁸

DISCUSSION

Changes in lysine methylation are orchestrated by the addition and removal of these methyl residues by methyltransferases

and demethylases. This equilibrium can be shifted by changes in an individual enzyme, as seen for other modified residues,²³ or can result from the collective changes brought about by multiple enzymes. It is also thought that an additional layer of complexity exists due to each enzyme regulating this modification only at specific loci within the genome, although the specific regions regulated by each methyltransferase and demethylase have not been identified. Together, these different layers of regulation and their dynamic changes within the cell can account for the global changes in H4K20Me3 across the entire genome.

Here, we provide the first evidence of differential regulation of histone H4K20 trimethylation in multiple models of cardiac dysfunction (summarized in the graphical abstract). Our results show an increase in H4K20 trimethylation in cultured cells subjected to pharmacologically induced acute hypertrophic stress, while mouse models of sustained cardiac dysfunction demonstrate a marked decrease. The differences between cell and animal models we observed may be due to the pro-hypertrophic agents used to treat the isolated cells: each pharmacological agent utilizes specific receptors to modulate hypertrophic pathways, which may not be comparable to a whole tissue response to cardiac dysfunction, such as that of the animal models we analyzed. Importantly, the animal models we examined represent a whole tissue response of two types of cardiac dysfunction, ischemic and NICM, which may be more similar to what occurs in human heart failure; however, histone H4K20 trimethylation has never been examined in human hearts. Thus, future studies would be necessary to assess changes in H4K20 trimethylation in human hearts experiencing heart failure.

To examine how this mark changes in response to disease over time, we measured changes in H4K20 trimethylation abundance throughout disease progression in ICM (48 h and 3 weeks post-ligation). While we found that there was no change detected at the early time point, we observed significant decreases in H4K20 trimethylation levels at 3 weeks post-ligation. These discrepancies in methylation abundance at different time points may be due to various reasons, including that 48 h post-ligation may not be sufficient to observe global histone H4K20 methylation abundance changes. It may also be due to the complex interplay between methyltransferases and demethylases in cardiac and non-cardiac cells within the heart that influence total H4K20 trimethylation abundance; however, this is beyond the scope of this publication.

Notably, H4K20 trimethylation has been primarily linked to gene repression (in non-cardiac cells), and our results suggests that this modification and the associated enzymes are key regulators of gene expression in cardiomyocytes during stress. Our results from animal models, showing a global decrease in this repressive histone modification after prolonged cardiac

dysfunction, are consistent with previous findings showing a global decrease in H3K9me3 (mark of gene repression) and increase in histone H3K4me3 (mark of gene activation).³⁹ Indeed, it has been suggested that global changes in gene expression patterns in cardiomyocytes may favor a more undifferentiated or fetal-like gene expression pattern,⁴⁰ often characterized by euchromatin, and enable the cell to dynamically adapt to stress. While this is the first study to correlate global changes in H4K20me3 abundance with the development of heart disease, additional analyses will be needed to identify the specific genes regulated by this PTM in the cardiomyocyte and their involvement in cardiac pathologies.

In addition, we identified two methyltransferases (KMT5A and SMYD5) and two demethylases (KDM7B and KDM7C) whose expression is altered in human heart failure patients. Of these four enzymes, only two have been examined in the heart previously. In the first study, the H4K20-specific methyltransferase was examined in the context of the heart, which showed that loss of SMYD5 in the developing zebrafish had no effect on cardiac development.³⁷ In the second study, KDM7B, the only H4K20-specific demethylase ever examined in the heart, was shown to be critical in regulating cardiac hypertrophy in a murine model of pressure overload.³⁶ No other studies have ever examined the other H4K20-specific methyltransferases and demethylases in the adult heart. Thus, future analyses will be necessary to elucidate regulatory functions of these enzymes in the context of heart failure.

One additional observation from our data is the decrease in total histone H4 levels seen by immunoblotting of cardiac tissue in both mouse models (albeit to varying degrees). Very few studies have reported dynamic changes in total histone protein levels, which have previously only been seen in non-cardiac cells.⁴¹ This discrepancy between histone H4 levels observed by immunoblotting versus mass spectrometry may be due to the impaired antibody binding caused by unknown neighboring histone PTMs. This phenomenon has been previously reported as a major challenge influencing antibody recognition for histones because of the presence of extensive modifications on histone tails; therefore, future studies may benefit from additional mass spectrometry analyses.³⁰

While this study is the first evaluation of H4K20me3 abundance in models of cardiac stress, two previous studies have reported changes in H4K20me3 in the cardiomyocyte during targeted analyses of specific pathways utilizing gain- and loss-of-function. The first study, by Oyama et al., showed that cardiac-specific deletion of heterochromatin protein 1 gamma (HP1 γ), which typically forms heterochromatin by associating with H3K9me3, had no effect on H3K9me3 levels but decreased H4K20me3 abundance in isolated cardiomyocytes.⁴² The second study, by Guan et al., investigated the TGF- β signaling pathway in cardiomyocytes and showed that TGF- β signaling leads to miR29-mediated inhibition of the methyltransferase Suv4-20h and resulted in decreased H4K20me3 and decreased cardiac function.⁴³ Thus, these studies begin to elucidate the possible mechanisms regulating H4K20me3 in the cardiomyocyte and further link decreased H4K20 trimethylation with cardiac dysfunction.

AUTHOR INFORMATION

Corresponding Authors

Samuel M. Hickenlooper – Nora Eccles Harrison
Cardiovascular Research and Training Institute, University of

Utah, Salt Lake City, Utah 84112, United States;
orcid.org/0000-0003-1535-7179; Phone: 801-581-8183;
Email: Samuel.hickenlooper@utah.edu; Fax: 801-581-3128

Sarah Franklin – Nora Eccles Harrison Cardiovascular
Research and Training Institute, University of Utah, Salt
Lake City, Utah 84112, United States; Division of
Cardiovascular Medicine, Department of Internal Medicine,
University of Utah School of Medicine, Salt Lake City, Utah
84132, United States; Email: sarah.franklin@utah.edu

Authors

Kathryn Davis – Nora Eccles Harrison Cardiovascular
Research and Training Institute, University of Utah, Salt
Lake City, Utah 84112, United States

Marta W. Szulik – Nora Eccles Harrison Cardiovascular
Research and Training Institute, University of Utah, Salt
Lake City, Utah 84112, United States

Hanin Sheikh – Nora Eccles Harrison Cardiovascular
Research and Training Institute, University of Utah, Salt
Lake City, Utah 84112, United States

Mickey Miller – Nora Eccles Harrison Cardiovascular
Research and Training Institute, University of Utah, Salt
Lake City, Utah 84112, United States

Steven Valdez – Nora Eccles Harrison Cardiovascular
Research and Training Institute, University of Utah, Salt
Lake City, Utah 84112, United States

Ryan Bia – Nora Eccles Harrison Cardiovascular Research
and Training Institute, University of Utah, Salt Lake City,
Utah 84112, United States

Complete contact information is available at:

<https://pubs.acs.org/10.1021/acsomega.2c00984>

Author Contributions

#S.M.H and K.D. contributed equally to this work. S.M.H, K.D., and S.F. came up with the concept of this manuscript; S.M.H. and S.F. designed the experiments; M.W.S., S.M.H., M.M., H.S., R.B, and S.V. performed the experiments and analyzed the data; K.D. and S.F. wrote the manuscript. All authors have read and approved the final version of the manuscript.

Notes

The authors declare no competing financial interest.

ACKNOWLEDGMENTS

This work was supported by the American Heart Association grant PRE35120356 and the Nora Eccles Harrison Treadwell Foundation grant 10038331.

REFERENCES

- (1) Virani, S. S.; Alonso, A.; Aparicio, H. J.; Benjamin, E. J.; Bittencourt, M. S.; Callaway, C. W.; Carson, A. P.; Chamberlain, A. M.; Cheng, S.; Delling, F. N.; et al. Heart Disease and Stroke Statistics-2021 Update: A Report From the American Heart Association. *Circulation* **2021**, *143*, e254–e743.
- (2) Blaxall, B. C.; Spang, R.; Rockman, H. A.; Koch, W. J. Differential myocardial gene expression in the development and rescue of murine heart failure. *Physiol. Genom.* **2003**, *15*, 105–114.
(a) Rockman, H. A.; Chien, K. R.; Choi, D. J.; Iaccarino, G.; Hunter, J. J.; Ross, J., Jr.; Lefkowitz, R. J.; Koch, W. J. Expression of a beta-adrenergic receptor kinase 1 inhibitor prevents the development of myocardial failure in gene-targeted mice. *Proc. Natl. Acad. Sci. U.S.A.* **1998**, *95*, 7000–7005. (b) Harding, V. B.; Jones, L. R.; Lefkowitz, R. J.; Koch, W. J.; Rockman, H. A. Cardiac beta ARK1 inhibition

prolongs survival and augments beta blocker therapy in a mouse model of severe heart failure. *Proc. Natl. Acad. Sci. U.S.A.* **2001**, *98*, 5809–5814.

(3) Kinugawa, K.; Minobe, W. A.; Wood, W. M.; Ridgway, E. C.; Baxter, J. D.; Ribeiro, R. C. J.; Tawadrous, M. F.; Lowes, B. A.; Long, C. S.; Bristow, M. R. Signaling Pathways Responsible for Fetal Gene Induction in the Failing Human Heart. *Circulation* **2001**, *103*, 1089–1094. (a) Parker, T. G.; Packer, S. E.; Schneider, M. D. Peptide growth factors can provoke "fetal" contractile protein gene expression in rat cardiac myocytes. *J. Clin. Invest.* **1990**, *85*, 507–514.

(4) Luger, K.; Mäder, A. W.; Richmond, R. K.; Sargent, D. F.; Richmond, T. J. Crystal structure of the nucleosome core particle at 2.8 Å resolution. *Nature* **1997**, *389*, 251–260.

(5) Huisinga, K. L.; Brower-Toland, B.; Elgin, S. C. The contradictory definitions of heterochromatin: transcription and silencing. *Chromosoma* **2006**, *115*, 110–122.

(6) Kouzarides, T. Chromatin Modifications and Their Function. *Cell* **2007**, *128*, 693–705.

(7) Allis, C. D.; Jenuwein, T. The molecular hallmarks of epigenetic control. *Nat. Rev. Genet.* **2016**, *17*, 487–500.

(8) Martin, C.; Zhang, Y. The diverse functions of histone lysine methylation. *Nat. Rev. Mol. Cell Biol.* **2005**, *6*, 838–849.

(9) Sims, R. J., 3rd; Nishioka, K.; Reinberg, D. Histone lysine methylation: a signature for chromatin function. *Trends Genet.* **2003**, *19*, 629–639. (a) Peters, A. H.; Mermoud, J. E.; O'Carroll, D.; Pagani, M.; Schweizer, D.; Brockdorff, N.; Jenuwein, T. Histone H3 lysine 9 methylation is an epigenetic imprint of facultative heterochromatin. *Nat. Genet.* **2002**, *30*, 77–80. (b) von Holt, C.; Brandt, W. F.; Greyling, H. J.; Lindsey, G. G.; Retief, J. D.; Rodrigues, J. d. A.; Schwager, S.; Sewell, B. T. [23] Isolation and characterization of histones. In *Methods Enzymology*; Wassarman, P. M., Kornberg, R. D., Eds.; Academic Press, 1989; Vol. 170, pp 431–523.

(10) DeLange, R. J.; Fambrough, D. M.; Smith, E. L.; Bonner, J. Calf and pea histone IV. II. The complete amino acid sequence of calf thymus histone IV; presence of epsilon-N-acetyllysine. *J. Biol. Chem.* **1969**, *244*, 319–334.

(11) Fang, J.; Feng, Q.; Ketel, C. S.; Wang, H.; Cao, R.; Xia, L.; Erdjument-Bromage, H.; Tempst, P.; Simon, J. A.; Zhang, Y. Purification and functional characterization of SET8, a nucleosomal histone H4-lysine 20-specific methyltransferase. *Curr. Biol.* **2002**, *12*, 1086–1099. (a) Nishioka, K.; Rice, J. C.; Sarma, K.; Erdjument-Bromage, H.; Werner, J.; Wang, Y.; Chuikov, S.; Valenzuela, P.; Tempst, P.; Steward, R.; et al. PR-Set7 is a nucleosome-specific methyltransferase that modifies lysine 20 of histone H4 and is associated with silent chromatin. *Mol. Cell* **2002**, *9*, 1201–1213. (b) Rice, J. C.; Nishioka, K.; Sarma, K.; Steward, R.; Reinberg, D.; Allis, C. D. Mitotic-specific methylation of histone H4 Lys 20 follows increased PR-Set7 expression and its localization to mitotic chromosomes. *Genes Dev.* **2002**, *16*, 2225–2230. (c) Schotta, G.; Lachner, M.; Sarma, K.; Ebert, A.; Sengupta, R.; Reuter, G.; Reinberg, D.; Jenuwein, T. A silencing pathway to induce H3-K9 and H4-K20 trimethylation at constitutive heterochromatin. *Genes Dev.* **2004**, *18*, 1251–1262.

(12) Shoaib, M.; Walter, D.; Gillespie, P. J.; Izard, F.; Fahrenkrog, B.; Lleres, D.; Lerdrup, M.; Johansen, J. V.; Hansen, K.; Julien, E.; et al. Histone H4K20 methylation mediated chromatin compaction threshold ensures genome integrity by limiting DNA replication licensing. *Nat. Commun.* **2018**, *9*, 3704.

(13) Hartlerode, A. J.; Guan, Y.; Rajendran, A.; Ura, K.; Schotta, G.; Xie, A.; Shah, J. V.; Scully, R. Impact of histone H4 lysine 20 methylation on 53BP1 responses to chromosomal double strand breaks. *PLoS One* **2012**, *7*, No. e49211. (a) Beck, D. B.; Oda, H.; Shen, S. S.; Reinberg, D. PR-Set7 and H4K20me1: at the crossroads of genome integrity, cell cycle, chromosome condensation, and transcription. *Genes Dev.* **2012**, *26*, 325–337.

(14) Jorgensen, S.; Schotta, G.; Sorensen, C. S. Histone H4 lysine 20 methylation: key player in epigenetic regulation of genomic integrity. *Nucleic Acids Res.* **2013**, *41*, 2797–2806. (a) Sanders, S. L.; Portoso, M.; Mata, J.; Bähler, J.; Allshire, R. C.; Kouzarides, T. Methylation of

histone H4 lysine 20 controls recruitment of Crb2 to sites of DNA damage. *Cell* **2004**, *119*, 603–614.

(15) Davis, K.; Azarcon, P.; Hickenlooper, S.; Bia, R.; Horiuchi, E.; Szulik, M. W.; Franklin, S. The role of demethylases in cardiac development and disease. *J. Mol. Cell. Cardiol.* **2021**, *158*, 89–100.

(a) Szulik, M. W.; Davis, K.; Bakhtina, A.; Azarcon, P.; Bia, R.; Horiuchi, E.; Franklin, S. Transcriptional regulation by methyltransferases and their role in the heart: highlighting novel emerging functionality. *Am. J. Physiol. Heart Circ. Physiol.* **2020**, *319*, H847–h865. (b) Southall, S. M.; Cronin, N. B.; Wilson, J. R. A novel route to product specificity in the Suv4-20 family of histone H4K20 methyltransferases. *Nucleic Acids Res.* **2014**, *42*, 661–671.

(16) Hyun, K.; Jeon, J.; Park, K.; Kim, J. Writing, erasing and reading histone lysine methylations. *Exp. Mol. Med.* **2017**, *49*, No. e324.

(17) Kaneda, R.; Takada, S.; Yamashita, Y.; Choi, Y. L.; Nonaka-Sarukawa, M.; Soda, M.; Misawa, Y.; Isomura, T.; Shimada, K.; Mano, H. Genome-wide histone methylation profile for heart failure. *Genes Cells* **2009**, *14*, 69–77.

(18) Franklin, S.; Chen, H.; Mitchell-Jordan, S.; Ren, S.; Wang, Y.; Vondriska, T. M. Quantitative analysis of the chromatin proteome in disease reveals remodeling principles and identifies high mobility group protein B2 as a regulator of hypertrophic growth. *Mol. Cell. Proteomics* **2012**, *11*, M111.014258.

(19) Movassagh, M.; Choy, M. K.; Knowles, D. A.; Cordeddu, L.; Haider, S.; Down, T.; Siggens, L.; Vujic, A.; Simeoni, I.; Penkett, C.; et al. Distinct epigenomic features in end-stage failing human hearts. *Circulation* **2011**, *124*, 2411–2422.

(20) Rau, C. D.; Wang, J.; Avetisyan, R.; Romay, M. C.; Martin, L.; Ren, S.; Wang, Y.; Lusic, A. J. Mapping genetic contributions to cardiac pathology induced by Beta-adrenergic stimulation in mice. *Circ.: Cardiovasc. Genet.* **2015**, *8*, 40–49.

(21) Chang, S. C.; Ren, S.; Rau, C. D.; Wang, J. J. Isoproterenol-Induced Heart Failure Mouse Model Using Osmotic Pump Implantation. *Methods Mol. Biol.* **2018**, *1816*, 207–220.

(22) Michael, L. H.; Entman, M. L.; Hartley, C. J.; Youker, K. A.; Zhu, J.; Hall, S. R.; Hawkins, H. K.; Berens, K.; Ballantyne, C. M. Myocardial ischemia and reperfusion: a murine model. *Am. J. Physiol.* **1995**, *269*, H2147–H2154.

(23) Warren, J. S.; Tracy, C. M.; Miller, M. R.; Makaju, A.; Szulik, M. W.; Oka, S. I.; Yuzyuk, T. N.; Cox, J. E.; Kumar, A.; Lozier, B. K.; et al. Histone methyltransferase Smyd1 regulates mitochondrial energetics in the heart. *Proc. Natl. Acad. Sci. U.S.A.* **2018**, *115*, E7871–E7880.

(24) Franklin, S.; Kimball, T.; Rasmussen, T. L.; Rosa-Garrido, M.; Chen, H.; Tran, T.; Miller, M. R.; Gray, R.; Jiang, S.; Ren, S.; et al. The chromatin-binding protein Smyd1 restricts adult mammalian heart growth. *Am. J. Physiol. Heart Circ. Physiol.* **2016**, *311*, H1234–H1247.

(25) Franklin, S.; Zhang, M. J.; Chen, H.; Paulsson, A. K.; Mitchell-Jordan, S. A.; Li, Y.; Ping, P.; Vondriska, T. M. Specialized compartments of cardiac nuclei exhibit distinct proteomic anatomy. *Mol. Cell. Proteomics* **2011**, *10*, M110.000703.

(26) Cox, J.; Hein, M. Y.; Lubner, C. A.; Paron, I.; Nagaraj, N.; Mann, M. Accurate proteome-wide label-free quantification by delayed normalization and maximal peptide ratio extraction, termed MaxLFQ. *Mol. Cell. Proteomics* **2014**, *13*, 2513–2526.

(27) Sucharov, C. C.; Mariner, P. D.; Nunley, K. R.; Long, C.; Leinwand, L.; Bristow, M. R. A β 1-adrenergic receptor CaM kinase II-dependent pathway mediates cardiac myocyte fetal gene induction. *Am. J. Physiol. Heart Circ. Physiol.* **2006**, *291*, H1299–H1308.

(28) Leenen, F. H. H.; White, R.; Yuan, B. Isoproterenol-induced cardiac hypertrophy: role of circulatory versus cardiac renin-angiotensin system. *Am. J. Physiol. Heart Circ. Physiol.* **2001**, *281*, H2410–H2416. (a) Ren, S.; Chang, S.; Tran, A.; Mandelli, A.; Wang, Y.; Wang, J. J. Implantation of an Isoproterenol Mini-Pump to Induce Heart Failure in Mice. *JoVE* **2019**, No. e59646.

(29) Regan, J. A.; Mauro, A. G.; Carbone, S.; Marchetti, C.; Gill, R.; Mezzaroma, E.; Valle Raleigh, J.; Salloum, F. N.; Van Tassel, B. W.; Abbate, A.; et al. A mouse model of heart failure with preserved

ejection fraction due to chronic infusion of a low subpressor dose of angiotensin II. *Am. J. Physiol. Heart Circ. Physiol.* **2015**, *309*, H771–H778.

(30) Fuchs, S. M.; Strahl, B. D. Antibody recognition of histone post-translational modifications: emerging issues and future prospects. *Epigenomics* **2011**, *3*, 247–249. (a) Fuchs, S. M.; Krajewski, K.; Baker, R. W.; Miller, V. L.; Strahl, B. D. Influence of Combinatorial Histone Modifications on Antibody and Effector Protein Recognition. *Curr. Biol.* **2011**, *21*, 53–58.

(31) Rattray, A. M.; Müller, B. The control of histone gene expression. *Biochem. Soc. Trans.* **2012**, *40*, 880–885.

(32) Kolk, M. V.; Meyberg, D.; Deuse, T.; Tang-Quan, K. R.; Robbins, R. C.; Reichenspurner, H.; Schrepfer, S. LAD-ligation: a murine model of myocardial infarction. *J. Visualized Exp.* **2009**, *32*, No. e1438.

(33) Sweet, M. E.; Cocciolo, A.; Slavov, D.; Jones, K. L.; Sweet, J. R.; Graw, S. L.; Reece, T. B.; Ambardekar, A. V.; Bristow, M. R.; Mestroni, L.; et al. Transcriptome analysis of human heart failure reveals dysregulated cell adhesion in dilated cardiomyopathy and activated immune pathways in ischemic heart failure. *BMC Genomics* **2018**, *19*, 812.

(34) Yang, K. C.; Yamada, K. A.; Patel, A. Y.; Topkara, V. K.; George, I.; Cheema, F. H.; Ewald, G. A.; Mann, D. L.; Nerbonne, J. M. Deep RNA sequencing reveals dynamic regulation of myocardial noncoding RNAs in failing human heart and remodeling with mechanical circulatory support. *Circulation* **2014**, *129*, 1009–1021.

(35) Liu, Y.; Morley, M.; Brandimarto, J.; Hannenhalli, S.; Hu, Y.; Ashley, E. A.; Tang, W. H.; Moravec, C. S.; Margulies, K. B.; Cappola, T. P.; et al. RNA-Seq identifies novel myocardial gene expression signatures of heart failure. *Genomics* **2015**, *105*, 83–89.

(36) Liu, X.; Wang, X.; Bi, Y.; Bu, P.; Zhang, M. The histone demethylase PHF8 represses cardiac hypertrophy upon pressure overload. *Exp. Cell Res.* **2015**, *335*, 123–134.

(37) Fujii, T.; Tsunesumi, S.; Sagara, H.; Munakata, M.; Hisaki, Y.; Sekiya, T.; Furukawa, Y.; Sakamoto, K.; Watanabe, S. Smyd5 plays pivotal roles in both primitive and definitive hematopoiesis during zebrafish embryogenesis. *Sci. Rep.* **2016**, *6*, 29157.

(38) Lee, J. H.; Gao, C.; Peng, G.; Greer, C.; Ren, S.; Wang, Y.; Xiao, X. Analysis of transcriptome complexity through RNA sequencing in normal and failing murine hearts. *Circ. Res.* **2011**, *109*, 1332–1341. (a) Gladka, M. M.; Molenaar, B.; de Ruiter, H.; van der Elst, S.; Tsui, H.; Versteeg, D.; Lacraz, G. P. A.; Huibers, M. M. H.; van Oudenaarden, A.; van Rooij, E. Single-Cell Sequencing of the Healthy and Diseased Heart Reveals Cytoskeleton-Associated Protein 4 as a New Modulator of Fibroblasts Activation. *Circulation* **2018**, *138*, 166–180. (b) Wang, J. J.; Rau, C.; Avetisyan, R.; Ren, S.; Romay, M. C.; Stolin, G.; Gong, K. W.; Wang, Y.; Lusis, A. J. Genetic Dissection of Cardiac Remodeling in an Isoproterenol-Induced Heart Failure Mouse Model. *PLoS Genet.* **2016**, *12*, No. e1006038.

(39) Franklin, S.; Chen, H.; Mitchell-Jordan, S.; Ren, S.; Wang, Y.; Vondriska, T. M. Quantitative analysis of the chromatin proteome in disease reveals remodeling principles and identifies high mobility group protein B2 as a regulator of hypertrophic growth. *Mol. Cell. Proteomics* **2012**, *11*, M111.014258.

(40) Kinugawa, K.; Minobe, W. A.; Wood, W. M.; Ridgway, E. C.; Baxter, J. D.; Ribeiro, R. C.; Tawadrous, M. F.; Lowes, B. A.; Long, C. S.; Bristow, M. R. Signaling pathways responsible for fetal gene induction in the failing human heart: evidence for altered thyroid hormone receptor gene expression. *Circulation* **2001**, *103*, 1089–1094.

(41) Lu, N. F.; Jiang, L.; Zhu, B.; Yang, D. G.; Zheng, R. Q.; Shao, J.; Yuan, J.; Xi, X. M. Elevated Plasma Histone H4 Levels Are an Important Risk Factor in the Development of Septic Cardiomyopathy. *Balk. Med. J.* **2020**, *37*, 72–78.

(42) Oyama, K.; El-Nachef, D.; Fang, C.; Kajimoto, H.; Brown, J. P.; Singh, P. B.; MacLellan, W. R. Deletion of HP1 γ in cardiac myocytes affects H4K20me3 levels but does not impact cardiac growth. *Epigenet. Chromatin* **2018**, *11*, 18.

(43) Lyu, G.; Guan, Y.; Zhang, C.; Zong, L.; Sun, L.; Huang, X.; Huang, L.; Zhang, L.; Tian, X.-L.; Zhou, Z.; et al. TGF- β signaling alters H4K20me3 status via miR-29 and contributes to cellular senescence and cardiac aging. *Nat. Commun.* **2018**, *9*, 2560.